PROCEEDINGS OF SCIENCE

Standard Model Effective-Field Theory in final states with multiple Higgs and gauge bosons

R. Covarelli[a,*]

[a] *Physics Department, Università di Torino and INFN,*
Via Pietro Giuria 1, Torino, Italy

E-mail: roberto.covarelli@unito.it

We analyze LHC processes involving interactions of two electroweak bosons and two Higgs bosons, VVHH, where V is a W or Z boson, in terms of their sensitivity to Standard Model Effective Field Theory (SMEFT) effects.

We examine the current experimental results of the CMS collaboration in the context of an 8-dimensional SMEFT. We show that the constraints arising from producing vector-boson-fusion Higgs pairs on the operators that modify the quartic gauge-Higgs interactions are already comparable to or more stringent than those published in the analysis of the vector-boson scattering processes using CMS. We study changes to such constraints when introducing perturbative unitarity bounds and investigate the potential for new experimental final states, such as associated production of ZHH. Finally, we show the prospects for the high-luminosity phase of the LHC.

The European Physical Society Conference on High Energy Physics (EPS-HEP2023)
21-25 August 2023
Hamburg, Germany

*Speaker

PoS(EPS-HEP2023)379

1. Introduction

Processes involving the scattering of multiple electro-weak (EW) as well as Higgs (H) at the Large Hadron Collider (LHC) can be regarded as powerful probes of beyond-the-Standard-Model (BSM) physics. In the Standard Model, electroweak symmetry breaking fixes the intensity of the VVH and VVHH interactions. Experimental measurement of possible deviations from the SM predictions in processes which feature such triple and quartic Higgs-gauge couplings (TCs and QCs) can then unravel deviations from the SM couplings in the EW gauge sector.

BSM scenarios can be described in a model-independent way by using an effective-field-theory (EFT) framework, in which indirect New Physics effects are parametrised by including in the Lagrangian higher-dimension operators. In the Standard Model EFT (SMEFT), operators affecting both TCs and QCs start at dimension 6 but, by only including dimension-6 effects, VVH and VVHH vertex factors remain completely correlated. Modifications of QCs with no TC contamination only arise in specific operators of dimension 8 or higher, which are called *genuine* anomalous quartic operators [1, 2].

We concentrate on the analysis of genuine SMEFT anomalous quartic operators, and set new constraints on their effects by means of VVHH interaction processes. The processes we consider are Higgs-pair production, both in vector-boson fusion mode (VBF-HH) and in association with a Z boson (ZHH). We also consider massive vector-boson-scattering (VBS) as benchmark processes for dimension-8 coefficient constraints.

We choose the subset of possible dimension-8 operators which modify VVHH vertex strengths [1, 2]. Among these operators, *scalar* (S) and *mixed* operators (M) can induce modifications of the VVHH vertex. Further details on the analysis can be found in [3].

2. Simulation setup and observables

The MadGraph5_aMC@NLO [4, 5] event generator at leading order (LO) in QCD, is used to simulate the aforementioned processes in proton-proton collisions at $\sqrt{s} = 13$ TeV. Table 1 lists the exact MadGraph5_aMC@NLO syntax and specific parameters used to generate the processes mentioned above.

EFT effects are simulated by loading suitable UFO models into MadGraph5_aMC@NLO for the entirety of the LO generation we used [9], a simulation of the loop-induced ggZZH process was also attempted and a dedicated UFO model at QCD NLO was built. Our simulations include sample sets with a Wilson coefficient f_X varied as $f_X/\Lambda^4 = 0$ up to ± 20 TeV^{-4} (X = S0-2, M0-7). In the VBF-HH studies at the LHC, the BSM effects are described in a different parameterization that is equivalent to inserting an effective VVHH vertex modifier κ_{2V}, where the SM corresponds to $\kappa_{2V} = 1$ [10] : sets of samples with an effective vertex factor $\kappa_{2V} = 0$ up to ± 10 are therefore also simulated.

In order to obtain a simplified estimate of the EFT sensitivity for different final states, we use the cross section as a physical observable (or equivalently the expected number of events observed at a given integrated luminosity) in the interval $m_{\text{min}} \leq m \leq m_{\text{max}}$, where m is the invariant mass of the dibosonic or tribosonic states produced in the various channels; we denote this cross section

Process number	MadGraph5_aMC@NLO syntax	QCD order	Max. jet flav.	CMS result	$\overline{\sigma}$[1.1, 13 TeV] SM (fb)
1	`p p > w+ w+ j j QCD=0` `p p > w- w- j j QCD=0`	LO	4	[6, 7]	4.514(9)
2	`p p > w+ z j j QCD=0` `p p > w- z j j QCD=0`	LO	4	[6, 7]	8.55(2)
3	`p p > w+ w- j j QCD=0`	LO	4	[7]	9.97(2)
4	`p p > h h j j QCD=0`	LO	5	[8]	0.0329(7)
5	`p p > z h h QED=3`	LO	5	-	0.01295(5)

Table 1: LHC processes of interest studied in the present work. The number of active flavours considered in protons and jets is also listed. $\overline{\sigma}[m_{\min}, m_{\max}]$ is the cross section in the interval $m_{\min} \leq m \leq m_{\max}$, with m being the invariant mass of the produced di- or tri-boson final state. Each cross-section value reports in brackets the integration uncertainty on the last digit. For VBS and VBF processes cuts on final-state jets are applied as: $m_{jj} > 500$ GeV, $|\Delta\eta_{jj}| > 2.5$.

as $\overline{\sigma}[m_{\min}, m_{\max}]$, or simply as $\overline{\sigma}$. An example of distribution of m in the presence or absence of EFT effects is presented in Figure **??** (on the left).

The unitarity limits for all operators are calculated as functions of f_X/Λ^4 using Ref. [2]. In all analyses presented below, $m_{\min}$ is set to a default value of 1.1 TeV.The choice is a compromise between the definition of a high-mass region enriched with EFT contributions, where SM backgrounds are negligible, and having a value $m_{\min}$ below the unitarity limit for the entire range of Wilson coefficients considered in analyses. The values of $\overline{\sigma}$ using $m_{\min} = 1.1$ TeV and $m_{\max} = \sqrt{s}$ (i.e. no upper limit) are shown in the figure rightmost column of the table 1.

3. Analysis of VBS processes

As a first step we show that constraints based solely on $\overline{\sigma}[m_{\min}, m_{\max}]$ are a reliable proxy of the actual EFT sensitivity, using experimentally known VBS processes. Initially we consider $m_{\max} = \sqrt{s}$, i.e. no unitarity constraint.

$\overline{\sigma}$ values are calculated for each simulated process and sample. The corresponding cross sections for a given experimental final state is obtained by multiplying $\overline{\sigma}$ by the branching fractions (BF) of the gauge and Higgs bosons involved. For the ZHH process, the mode H$\to$ b$\bar{\text{b}}$, Z $\to \ell^+\ell^-$ is chosen.

The cross sections for each channel are calculated as functions of f_X/Λ^4, and quadratic fits are performed on the obtained results. An experimental CMS analysis is selected and the published 95% CL exclusion limit is considered on a randomly chosen operator coefficient. The exclusion limit is imposed on the parabola corresponding to the chosen operator, obtaining a CL exclusion limit of 95% on $\overline{\sigma}$, from which the exclusion limits on the corresponding coefficients are in turn determined. The limits obtained with this procedure are systematically compared with those published by the CMS. We observe that validation is everywhere success except for operators S0-2 in CMS WV semileptonic analysis, where validation results are slightly more pessimistic than published values.

To consider the limits of unitarity in the limits, we adopt a "clipping" method, following a similar approach to the one in Refs. [11–13]. In our approach, we evaluate $\overline{\sigma}[m_{\text{min}}, m_{\text{max}}]$ for different values of m_{max}, varying between $m_{\text{min}} + 100$ GeV and the maximum kinematically allowed mass. In an experimental analysis, this approach would be equivalent to not considering data or simulated events greater than m_{max} in the measurement. For each of these values of $\overline{\sigma}$, the procedure used for validation is followed to obtain the m_{max} dependent bounds on the operator coefficients.

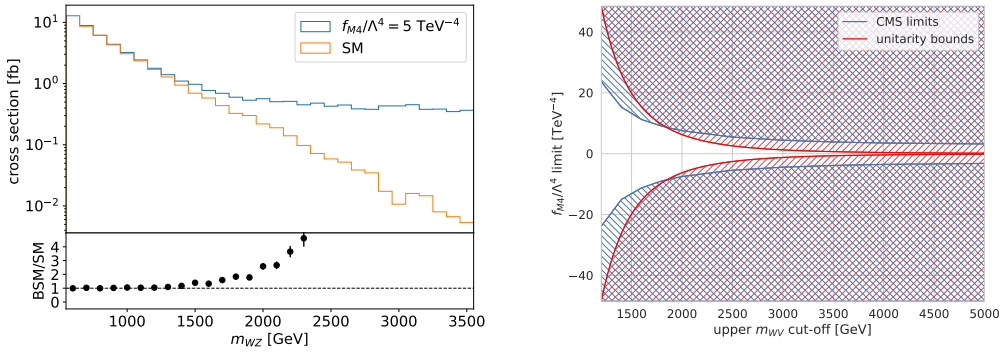

Figure 1: f_{M4} operator: Invariant mass distributions for the VBS WZ process (left) and estimated limits for the VBS W$^{\pm}$V semileptonic process, as a function of the upper invariant mass cut-off m_{max} (right). Superimposed are the unitarity bounds (red lines). The intersection of the experimental and the unitarity-bound curves represents the best limits which can unambiguously be interpreted in an EFT expansion without violating unitarity.

Fig. 1 (right) shows examples of m_{max}-dependent bounds for specific processes and operators. For large m_{max} the experimental limits without unitarity are recovered, while the limits become less stringent for values smaller than m_{max} due to the reduced statistics of the data and the weaker dependence of $\overline{\sigma}$ on the operator coefficient in narrower ranges. Unitarity bounds derived from [2] are also shown. The intersection of the experimental and unitarity curves represents the maximum invariant mass and the corresponding limit on f_X/Λ^4 that can be interpreted unambiguously in an EFT expansion without violating unitarity.

4. Analysis of the VBF-HH process

As mentioned above, the experimental results for VBF-HH are expressed in terms of an effective vertex factor VVHH, $\kappa_{2\text{V}}$, instead of as limits on EFT Wilson coefficients. We use a similar procedure to the one used for VBS validation, using the published CL exclusion limit of 95%, impose an exclusion limit on $\overline{\sigma}$ from the corresponding parabola using simulation, and finally determining the exclusion limits on the Wilson coefficients.

In Table 2 we present the relevant upper limits without regularization of unitarity, compared to the best bounds found using VBS analysis in Section 3. Despite the much smaller cross-sections, we already find that, with available LHC data, estimated VBF-HH limits supersede those obtained with VBS for f_{M0}, f_{M2} and f_{M3} and are mostly comparable for all other M-type operators.

A similar procedure is followed to obtain limits that take into account unitarity. In Table 2 we also present the relevant upper bounds with regularization of unitarity, with respect to the best

	VBS $W^{\pm}V$ semileptonic		VBF HH$\rightarrow b\bar{b}b\bar{b}$	
Coeff.	no unitarity	w/ unitarity	no unitarity	w/ unitarity
f_{M0}/Λ^4	[-1.0,1.0]	[-3.3,3.5]	[-0.95,0.95]	[-3.3,3.3]
f_{M1}/Λ^4	[-3.1,3.1]	[-7.4,7.6]	[-3.8,3.8]	[-13,14]
f_{M2}/Λ^4	[-1.5,1.5]	[-9.1,9.0]	[-1.3,1.3]	[-7.6,7.3]
f_{M3}/Λ^4	[-5.5,5.5]	[-32,30]	[-5.2,5.3]	[-29,30]
f_{M4}/Λ^4	[-3.1,3.1]	[-8.6,8.7]	[-4.0,4.0]	[-14,14]
f_{M5}/Λ^4	[-4.5,4.5]	[-10,10]	[-7.1,7.1]	[-26,26]
f_{M7}/Λ^4	[-5.1,5.1]	[-11,11]	[-7.6,7.6]	[-27,27]
f_{S0}/Λ^4	[-4.2,4.2]	[-8.5,9.5]	[-30,29]	/
f_{S1}/Λ^4	[-5.2,5.2]	/	[-11,10]	/
f_{S2}/Λ^4	-	[-21,25]	[-17,16]	/

Table 2: Comparison between VBF-HH constraints and those obtained from semileptonic VBS with or without unitarity constraints, with limits extracted from current CMS Run2 analyses. All entries represent 95% CL lower and upper limits in units of TeV^{-4}. Bars represent processes for which there is no sensitivity to the corresponding operator, or cases where the theoretical unitarity bound is more stringent than the experimental one for all m_{max} cut-off values.

limits found using VBS analysis in Section 3. The result for f_{M3} is shown in Figure 2 (black and red lines). The conclusions of the previous paragraph remain valid.

5. New experimental final states

The ZHH process, not yet studied in dedicated experimental analyses, is considered. The purpose is to investigate the potential sensitivity by performing an exploratory feasibility study.

For the ZZH process, we consider the LHC Run2 luminosity and we estimate the number of detectable events as $N = \overline{\sigma} \cdot \mathcal{L} \cdot \varepsilon \cdot A$, where A denotes the experimental acceptance for the Z and H decay products and ε is the corresponding total detection efficiency. We compute values of $\overline{\sigma}$ for the signal as in Section 2, by assuming the Higgs boson decaying into a $b\bar{b}$ pair, and the Z bosons decaying into leptons (electrons and muons). We generate the $pp \rightarrow Zb\bar{b}b\bar{b}$ SM process, which represents the dominant background in this final state, and cuts on the invariant mass of the b quark-antiquark pairs are applied to have them close to the nominal H mass.

From the derived estimates of the signal and background yields, we compute 95% CL upper limits on the cross section of the ZHH process using the Feldman-Cousins approach [14], and then we use this result to evaluate the limits on EFT operators with a procedure analogous to those presented in the previous sections, taking into account unitarity regularisation. No valid limits are found in presence of unitarity with Run2 luminosity.

6. Perspectives for HL-LHC

In the absence of unitary regularization and assuming Poissonian scaling in statistically dominated high-mass regions, the 95% CL exclusion bounds on $\overline{\sigma}$ are predicted to improve as $\mathcal{L}^{-1/2}$,

	VBS $W^{\pm}V$ semileptonic		VBF HH→ $b\bar{b}b\bar{b}$	
Coeff.	no unitarity	w/ unitarity	no unitarity	w/ unitarity
f_{M0}/Λ^4	[-0.47,0.47]	[-0.96,1.02]	[-0.43,0.43]	[-0.90,0.87]
f_{M1}/Λ^4	[-1.5,1.5]	[-2.3,2.4]	[-1.7,1.7]	[-3.5,3.5]
f_{M2}/Λ^4	[-0.69,0.68]	[-2.1,2.1]	[-0.62,0.61]	[-1.7,1.7]
f_{M3}/Λ^4	[-2.5,2.4]	[-6.8,6.3]	[-2.4,2.4]	[-6.5,6.6]
f_{M4}/Λ^4	[-1.4,1.4]	[-2.4,2.5]	[-1.8,1.8]	[-3.9,4.0]
f_{M5}/Λ^4	[-2.0,2.0]	[-3.0,3.1]	[-3.2,3.2]	[-6.9,7.0]
f_{M7}/Λ^4	[-2.4,2.4]	[-3.5,3.5]	[-3.5,3.5]	[-7.1,7.1]
f_{S0}/Λ^4	[-1.8,2.0]	[-2.6,3.3]	[-14,13]	/
f_{S1}/Λ^4	[-2.4,2.4]	[-5.8,6.1]	[-5.1,4.5]	/
f_{S2}/Λ^4	[-2.3,2.4]	[-4.8,5.2]	[-8.1,7.1]	/

Table 3: Comparison of VBF-HH constraints with those obtained from VBS when applying or not unitarity constraints, in a projection with full HL-LHC luminosity. All entries represent 95% CL lower and upper limits in units of TeV^{-4}. Bars represent processes for which there is no sensitivity to the corresponding operator, or cases where the theoretical unitarity bound is more stringent than the experimental one for all m_{max} cut-off values.

with $\mathcal{L}$ being the integrated luminosity. From the dependence of the cross section on the Wilson coefficients is quadratic, the related f_X/Λ^4 limits scale as $\mathcal{L}^{-1/4}$, producing a very slight improvement of a factor of about 2.2, when moving from 140 fb^{-1} of the LHC Run2 to the 3000 fb^{-1} expected from the HL-LHC.

In contrast, bounds in presence of unitarity gain significantly from an increase in the data set, since the value m_{max} for which the result remains interpretable by the EFT shifts correspondingly to larger values, allowing more data to be included in the sensitivity estimate. This effect would lead to improvements on the limits by factors up to 4-5, as shown for f_{M3} in Figure 2.

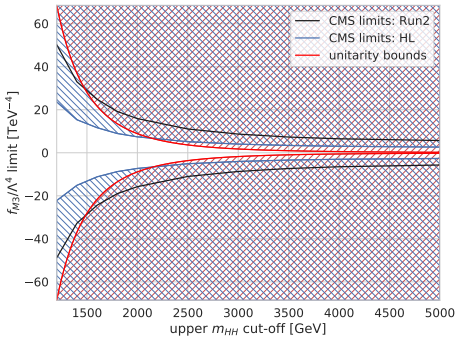

Figure 2: Estimated limits on the f_{M3} Wilson coefficient in VBF-HH as a function of the upper invariant mass cut-off m_{max}. Black lines represent the current Run2 scenario (140 fb^{-1}) while blue lines represent the HL-LHC scenario (3000 fb^{-1}). Superimposed are the unitarity bounds derived from [2] (red line). While all individual results scale roughly as $\mathcal{L}^{-1/4}$, the improvement on the EFT-interpretable limit is a factor of 4.6.

References

[1] O.J.P. Eboli, M.C. Gonzalez-Garcia and J.K. Mizukoshi, *$p\,p \to j\,j\,e^{\pm}\,\mu^{\pm}\nu\nu$ and $j\,j\,e^{\pm}\,\mu^{\pm}\nu\nu$ at $O(\alpha_{em}^6)$ and $O(\alpha_{em}^4\alpha_s^2)$ for the study of the quartic electroweak gauge boson vertex at CERN LHC*, *Phys. Rev. D* **74** (2006) 073005 [hep-ph/0606118].

[2] E.d.S. Almeida, O.J.P. Éboli and M.C. Gonzalez–Garcia, *Unitarity constraints on anomalous quartic couplings*, *Phys. Rev. D* **101** (2020) 113003 [2004.05174].

[3] A. Cappati, R. Covarelli, P. Torrielli and M. Zaro, *Sensitivity to new physics in final states with multiple gauge and Higgs bosons*, *JHEP* **09** (2022) 038 [2205.15959].

[4] J. Alwall, R. Frederix, S. Frixione, V. Hirschi, F. Maltoni, O. Mattelaer et al., *The automated computation of tree-level and next-to-leading order differential cross sections, and their matching to parton shower simulations*, *JHEP* **07** (2014) 079 [1405.0301].

[5] R. Frederix, S. Frixione, V. Hirschi, D. Pagani, H.S. Shao and M. Zaro, *The automation of next-to-leading order electroweak calculations*, *JHEP* **07** (2018) 185 [1804.10017].

[6] CMS collaboration, *Measurements of production cross sections of WZ and same-sign WW boson pairs in association with two jets in proton-proton collisions at $\sqrt{s}$ = 13 TeV*, *Phys. Lett. B* **809** (2020) 135710 [2005.01173].

[7] CMS collaboration, *Search for anomalous electroweak production of vector boson pairs in association with two jets in proton-proton collisions at 13 TeV*, *Phys. Lett. B* **798** (2019) 134985 [1905.07445].

[8] CMS collaboration, *Search for Higgs Boson Pair Production in the Four b Quark Final State in Proton-Proton Collisions at $\sqrt{s}$=13 TeV*, *Phys. Rev. Lett.* **129** (2022) 081802 [2202.09617].

[9] https://feynrules.irmp.ucl.ac.be/wiki/AnomalousGaugeCoupling.

[10] F. Bishara, R. Contino and J. Rojo, *Higgs pair production in vector-boson fusion at the LHC and beyond*, *Eur. Phys. J. C* **77** (2017) 481 [1611.03860].

[11] J. Kalinowski, P. Kozów, S. Pokorski, J. Rosiek, M. Szleper and S. Tkaczyk, *Same-sign WW scattering at the LHC: can we discover BSM effects before discovering new states?*, *Eur. Phys. J. C* **78** (2018) 403 [1802.02366].

[12] P. Kozów, L. Merlo, S. Pokorski and M. Szleper, *Same-sign WW Scattering in the HEFT: Discoverability vs. EFT Validity*, *JHEP* **07** (2019) 021 [1905.03354].

[13] G. Chaudhary, J. Kalinowski, M. Kaur, P. Kozów, K. Sandeep, M. Szleper et al., *EFT triangles in the same-sign WW scattering process at the HL-LHC and HE-LHC*, *Eur. Phys. J. C* **80** (2020) 181 [1906.10769].

[14] G.J. Feldman and R.D. Cousins, *A Unified approach to the classical statistical analysis of small signals*, *Phys. Rev. D* **57** (1998) 3873 [physics/9711021].